Two Years of Continuous Measurements of Tidal and Nontidal Variations of Gravity in Boulder, Colorado

Tonie M. van Dam and Olivier Francis[1]

NOAA/NGS and CIRES, University of Colorado, Boulder

Abstract. We report here on the results of an analysis of 2 years of data from NOAA's superconducting gravimeter located at the Table Mountain Gravity Observatory in Boulder, Colorado. Observed tidal parameters, corrected for ocean loading effects, are compared with theoretical tidal parameters predicted for a non-hydrostatic inelastic Earth model and demonstrate excellent agreement. Tidal residuals, corrected for polar motion and a linear instrument drift are highly correlated with gravity changes measured by two absolute gravimeters over the same time period. The admittance to local pressure is found to be -0.356 µGal/mbar. However, this admittance factor is found to be seasonally and frequency dependent. Correlations between rainfall events and gravity changes are observed. Attempts to model these gravity changes as exponential functions of time were unsuccessful.

Introduction

Gravity changes at the Earth's surface result from elevation changes, redistributions of mass below the surface, oceanic or atmospheric loading, changes in the relative positions of celestial bodies, and from changes in the rotation rate or the position of the rotation axis of the Earth. Continuous measurements of gravity can, therefore, provide information about a variety of geophysical processes.

In April of 1995, the National Oceanic and Atmospheric Administration (NOAA), as part of their Climate and Global Change Program, installed a GWR compact style superconducting gravimeter [*Warburton and Brinton*, 1995] at their Table Mountain Gravity Observatory (TMGO) near Boulder, Colorado. The relative gravimeter, C024, is capable of detecting sub-microgal gravity variations. In this paper, we report on the analysis of more than 2 years of data collected by C024. We consider the effects of Earth tides, polar motion, atmospheric pressure, and rainfall on the gravity measurements. We compare the superconducting gravimeter (SG) residuals with episodic absolute gravity observations from the same site over the two year time period.

Calibration

The output of the SG is the voltage in the feedback coil of the instrument required to maintain a niobium sphere levitating in a magnetic field in a neutral position. This voltage is converted into a gravitational acceleration by calibrating the SG with known or measured gravity changes. C024 was calibrated by fitting its output voltages to data obtained simultaneously by a second SG owned by the Institute for Applied Geodesy (IfAG). The IfAG instrument operated at

TMGO from April 1995 to July 1996 and was itself calibrated using an acceleration platform [see *Richter*, 1995]. The calibration factor for C024 is -80.341 ± .01 μGal/volt. The IfAG instrument operated at TMGO for one year and was itself calibrated using an acceleration platform [see *Richter*, 1995]. The calibration factor for C024 is -80.341 ± .009 μGal/volt. This result is consistent with the calibration factor of -80.281 ± .063 μGal/volt determined by fitting the SG voltages to gravity changes observed with a collocated FG5 absolute gravimeter.

Earth Tide Analysis

The SG records data continuously with a data sampling rate of 5 seconds. Spikes were removed and the data filtered to one minute, the sampling rate of the environmental parameters. Data gaps, earthquakes and tares were removed using *TSoft*, an interactive graphical software package for the analysis of Earth tides [*P. Vauterin*, personal communication]. Only 4 tares, associated with power outages and helium refilling, were identified. The edited data were filtered to one hour. Tidal parameters were estimated with the ETERNA package [*Wenzel*, 1996]. The values of the tidal parameters were obtained using the instrumental phase lag of 37 seconds, based on the manufacturer's specifications for the electronics. The instrumental phase lag for C024 is known to about 3% (R. Warburton, personal communication) which would introduce an error into the phases of M_2 of approximately 2%.

Figure 1a compares the amplitude of the gravimetric tidal factors in the diurnal band with the nearly diurnal free wobble resonance curve for a non-hydrostatic inelastic Earth model [*Dehant, V., P. Defraigne, and J. Wahr*, Tides for a convective Earth, unpublished manuscript]. While the estimated parameters agree well with the predicted resonance curve, they are still systematically higher than the values predicted by the model.

Adjusting the tidal parameters for ocean loading, substantially improves the fit between the observations and the model. Diurnal ocean loading effects are large in the western US due to the tidal resonance in the Northwest Pacific ocean (compare the amplitude of the loading of $K_1 \approx 0.2$ μGal in Northern Europe to $K_1 \approx 1.3$ μGal in Boulder). Three tidal models were compared: CSR3.0 [*Eanes and Bettadpur*, 1995], FES95.2 [*Le Provost et al*., 1994] and Schwiderski [*Schwiderski*, 1980; 1983]. The ocean loading estimates from CSR3.0 and FES95.2 demonstrated the greatest improvement and are shown in Figure 1a.

In Figure 1b we compare the delta factors in the semi-diurnal band corrected and uncorrected for ocean loading effects with the Earth tide model. Again, correcting for ocean loading effects improves the fit to the model, when ocean tide models are available.

Atmospheric Pressure

ETERNA allows the simultaneous determination of the tidal parameters and the local air pressure admittance factor by least squares adjustment. An admittance of -0.356 ± 0.001

μGal/mbar was determined. This value is significantly larger than the modeled admittance for Boulder of -0.31 ± 0.01 μGal/mbar, calculated by taking the ratio of the gravity effect, determined by convolving *Farrell's* [1972] elastic Green's functions with global pressure data [*van Dam and Wahr*, 1987], and the local atmospheric pressure.

Empirical determinations of the admittance agree with the current value to within the error bars. For example, *Niebauer et al.* [1988] determined the admittance to be -0.36 ± 0.02 μGal/mbar using one month of absolute gravity data. *Levine et al*. [1986] obtained a value of -0.39 ± 0.04 μGal/mbar using a spring tidal gravimeter.

Still there is some variability in the observed admittances. To try to understand this variability, we used ETERNA to determine the admittance for each separate month of data (solid circles, Figure 2a). The admittance varies between a low of -0.327 ± 0.003 μGal/mbar in the winter and a high in the summer of -0.383 ± 0.007 μGal/mbar.

The higher admittance in the summer probably indicates that the local pressure does not characterize the regional pressure field well at this time of year. Gravity changes result from 1) a changing atmospheric mass and 2) the associated surface deformation. The deformation effect is maximized when the load is coherent over large distances as happens in the winter [*Whittaker and Horn*, 1981; *Zishka and Smith*, 1980]. Since the deformation is in the opposite sense to the mass attraction, the admittance is reduced during the winter. If the deformation effects were removed from the data, then the admittance to pressure should be fairly constant over the entire year. This is indeed what we find. The open squares in Figure 2a are the monthly admittances recalculated after first removing the predicted deformation effect from the gravity data. The deformation effect to gravity was estimated using 12-hourly global NMC surface pressure data convolved with *Farrell's* [1972] Green's functions [*van Dam and Wahr*, 1987]. We currently only have atmospheric pressure data through February, 1997. The admittance still displays some seasonal variability but not as much as the values not corrected for the deformation effect.

The results in Figure 2a indicate that the admittance to the atmospheric mass effect is -0.37 μGal/mbar, not -0.42 μGal/mbar, the value expected by modeling the local atmospheric mass change by an infinite half-space of air. Some reduction in the theoretical admittance is expected since the infinite half-space model ignores the scale height of the atmosphere. Taking this into account, *Niebauer* [1987] estimated that the admittance at Boulder should be approximately -0.40 μGal/mbar. The further reduction that we observe may be the result of the local geography since TMGO is located on a mesa and there may be a significant amount of local atmospheric mass below the instrument.

The pressure admittance also displays a frequency dependence. These results are shown in Figure 2b. There is a low admittance at periods of 1,2,3, and 4 cycles per day similar to that found by *Merriam* [1993] and *Crossley et al.* [1995] for the SG site in Canada. The decreased admittance for frequencies less 0.5 cycle/day again may indicate that local pressure does not reliably predict the long wavelength characteristic of the pressure field at these frequencies.

Polar Motion and Instrument Drift

Figure 3 shows the gravity residuals, with tides and atmospheric pressure effects removed, filtered to daily values. The residuals display two characteristic features, a long period sinusoidal variability associated with polar motion and a long term trend. We estimate the polar motion effect using the formulation of *Wahr* [1985]. Polar motion effects, determined using International Earth Rotation Service daily estimates of the pole position, are also plotted in Figure 3. A long term trend has been added to the polar motion model for visual clarity.

After removing the effects of polar motion, there is still a significant trend in the data. This trend is related to the long term drift of the instrument. We fit a line to the residuals to remove this effect. The line has a slope of 7.87 ± .08 μGal/yr.

Long Term Gravity Change

The SG residuals (observations corrected for tides, air pressure, polar motion and long term drift) are shown in Figure 4. A periodic signal remains in the data. This annual signal is most likely due to unmodeled environmental signals such as hydrology, non-tidal ocean loading, and atmospheric pressure which all have peak-to-peak annual signals of 1-3 μGals.

We compare these SG residuals with absolute gravity observations. This is the only SG site in the world where absolute gravity has regularly been observed for such an extensive period. NOAA maintains and deploys 2 FG5 absolute gravimeters, #102 purchased by NOAA for internal use and #111 purchased by the NSF for use by the US academic community [see *Bilham and Sasagawa*, 1994]. Both instruments are used extensively in the field and hence measurements at TMGO are done as the opportunities present themselves.

The absolute gravity data, corrected for Earth and ocean tides, atmospheric pressure effects and polar motion are shown in Figure 4. (TMGO has 9 absolute gravity sites. However, only data from pier AG are shown to eliminate systematic effects in the absolute gravity results due to horizontal and vertical gravity gradients.) In general, the SG residuals track changes in gravity observed with the collocated absolute gravimeters. Given that the two systems are not affected by similar systematic errors, the observed correlation indicates that the SG at Boulder is registering real changes in gravity and is not due to instrumental effects once a linear drift is removed.

Rainfall

The large increase in gravity observed immediately after the installation of C024, is most likely related to a period of anomalous rainfall in Boulder. Daily rainfall data for the state of Colorado are collected and archived by the State Climatological Office in Fort Collins. Rainfall data from Longmont are shown in Figure 5 (TMGO is located approximately 10 km from this rain gauge). There appears to be a correlation between the rainfall events and increases in gravity, especially during the spring of 1995. However, there are also instances where an increase in rainfall is followed by a decrease in gravity, i.e. the middle of 1997. The apparently anomalous response of gravity to rainfall at this time could be related to the fact that the Longmont rain gauge does not always reliably predict the rainfall at TMGO or that additional factors such as temperature, relative humidity, and soil moisture may also be important in determining the relationship between rainfall and gravity changes.

Ad hoc models that relate increases in gravity to rainfall as an exponential function of time were tested using a number of decay constants [see *Richter*, 1995; *Goodkind*, 1990; *Klopping et al*., 1995]. However, these models were only moderately successful in Boulder. Changes in gravity are more dependent on the amount of water in the soil beneath the gravity meter than in the height of a sheet of water on the surface. A soil moisture gauge is currently being installed at TMGO. It is hoped that a well for monitoring the level of the of water table will also be drilled soon. These data, temperature and relative humidity data, in addition to the rainfall data will be much more useful for constraining the relationship between the hydrology and the observed gravity changes than rainfall alone.

Conclusion

More than two years of SG data from Boulder, Colorado have been analyzed. The residuals, in general, track simultaneous measurements of absolute gravity from the same site. This correlation provides confidence that the gravity changes being observed with C024 are environmentally or geophysically driven. Anomalous signals in the residuals are most likely related to unmodeled environmental effects such as the atmosphere, hydrology, or non-tidal ocean loading.

Acknowledgments. We would like to thank P. Vauterin and M. Hendrickx for their assistance in processing the SG data. We would also like to thank G. Sasagawa for processing and providing the FG5 data. We are grateful to an anonymous reviewer whose thoughtful comments improved the quality of this paper. Finally, we would like to thank the Royal Observatory of Belgium for hosting one of the authors, T. van Dam, while this work was being completed.

References

Bilham, R., G. Sasagawa, U.S. geoscience community gains an absolute gravimeter, *EOS Trans. of AGU, 75*, 569-570, 1994.

Crossley, D.J., O.G. Jensen, J. Hinderer, Effective barometric admittance and gravity residuals, *Phys. Earth Planet. Int., 90*, 221-241, 1995.

Eanes, R. and S. Bettadpur, The CSR 3.0 global ocean tide model, *Technical Mem., CSR-TM-95-06*, Center for Space Research, Austin, Texas, 1995.

Farrell, W.E., Deformation of the Earth by surface loads, *Rev. of Geophys. 10*, 761-797, 1972.

Goodkind, J., C. Young, Gravity and hydrology at Kilauea volcano, the geysers, and Miami, in workshop proceedings, Non-tidal gravity changes, *Proc. of Workshop: Non-tidal gravity changes, Cahiers du Centre Européen de Géodynamique et de Séismologie, 3*, 163-167, 1990.

Klopping, F.J., G. Peter, K. Berstis and W.E. Carter, Analysis of two 525 day long data sets obtained with two side-by-side simultaneously recording superconducting gravimeters at Richmond Florida, USA, *Proc. of Second Workshop: Non-tidal gravity changes, Cahiers du Centre Européen de Géodynamique et de Séismologie*, *11*, 57-69, 1995.

Le Provost, C., L. Genco, F. Lyard, P. Vincent, and F. Rabilloud, Spectroscopy of the world ocean tides from a finite element hydrodynamic model, *J. Geophys. Res.*, *99*, 24,777-24,797, 1994.

Levine, J., J.C. Harrison, and W. Dewhurst, Gravity tide measurements with a feedback gravity meter, *J. Geophys. Res., 91*, 12,835-12,841,1986.

Merriam, J.B., The atmospheric pressure correction in gravity at Cantley, Quebec, *Proc. of the 12th International Symposium on Earth Tides*, 161-168, 1993.

Niebauer, T., Correcting gravity measurements for the effects of local air pressure, *J. Geophys. Res.*, *93*, 7989-7991, 1988.

Niebauer, T., New absolute gravity instruments for physics and geophysics, Ph.D. thesis, 155 pp., University of Colorado at Boulder, November 1987.

Richter, B., Cryogenic gravimeters: Status report on calibration, data acquisition, and environmental effects, *Proc. of Second Workshop: Non-tidal gravity changes, Cahiers du Centre Européen de Géodynamique et de Séismologie*, *11*, 125-146, 1995.

Schwiderski, E.W., Ocean tides: I. Global ocean tidal equations; II A hydrodynamic interpolation model, *Marine Geodesy, 3*, 161-217 and 219-255, 1980.

Schwiderski, E.W., Atlas of ocean tidal charts and maps. I: The semi-diurnal principal lunar tide M_2, *Marine Geodesy, 6*, 219-265, 1983.

van Dam, T., and J.M. Wahr, Displacements of the Earth's surface due to atmospheric loading: Effects on gravity and baseline measurements, *J. Geophys. Res*, *92*, 1282-1286, 1987.

Warburton, R.J. and E.W. Brinton, Recent Developments in GWR Instrument's superconducting Gravimeters, in workshop proceedings, Non-tidal gravity changes, *Proc. of Second Workshop: Non-tidal gravity changes, Cahiers du Centre Européen de Géodynamique et de Séismologie*, *11*, 23-56, 1995.

Wahr, J., Deformation induced by polar motion, *J. Geophys. Res., 90*, 9363-9368, 1985.

Wenzel, H.-G., The nanogal software: Earth tide data processing package, ETERNA 3.30, *Bulletin d'Information Marées Terrestres*, *124*, 9425-9439, 1996.

Whittaker, L.M. and L.H. Horn, Geographical and seasonal distribution of North American cyclogenesis, 1958-1977, *Monthly Weather Rev.*, *109*, 2312-2322. 1981.

Zishka, K.M. and P.J. Smith, The climatology of cyclones and anticyclones over North America and surrounding ocean environs for January and July, 1950-1977, *Monthly Weather Rev.*, *108*, 387-401, 1980.

O. Francis and T. van Dam, NOAA/NGS and CIRES, University of Colorado, Boulder, CO 80309. (e-mail: olivier@robeson.colorado.edu, tonie@robeson.colorado.edu)

(Received September 15, 1997; revised December 9, 1997; accepted December 16, 1997.)

---

[1]Permanent affiliation: Observatoire Royal de Belgique, Bruxelles, Belgium.

Figure 1. Comparisons of estimated diurnal tidal parameters with Nearly Diurnal Free Wobble model for a non-hydrostatic inelastic Earth (solid line). Delta factors uncorrected (circles) and corrected (CSR3.0 model = squares; FES95.2 = diamonds) for ocean loading effect versus model. a) Comparison in the diurnal band. b) Comparison in the semi-diurnal band.

Figure 2. Pressure admittance. a) Solid circles represent the admittance calculated for each month of data using ETERNA. Admittance is higher in the summer. Open squares represent the admittances recalculated after first removing the effects of deformation from the SG data. b) Admittance as a function of frequency.

Figure 3. Tidal gravity residuals (solid line) and estimated polar motion (dotted line). A drift of 7.87 μGal/yr was added to the polar motion model for visual clarity.

Figure 4. Superconducting Gravimeter residuals versus FG5 determinations of gravity change. Residuals corrected for tides, polar motion, and linear drift. Circles represent data taken from the NOAA instrument; Squares from the NSF instrument.

Figure 5. Comparison of gravity residuals (solid line) with rainfall events (dotted line).

Figure 1. Comparisons of estimated diurnal tidal parameters with Nearly Diurnal Free Wobble model for a non-hydrostatic inelastic Earth model (solid line). Delta factors uncorrected (circles) and corrected (CSR3.0 model = squares; FES95.2 = diamonds) for ocean loading effect versus model. a) Comparison in the diurnal band. b) Comparison in the semi-diurnal band.

Figure 2. Pressure admittance. a) Solid circles represent the admittance calculated for each month of data using ETERNA. Admittance is higher in the summer. Open squares represent the admittances recalculated after first removing the effects of deformation from the SG data. b) Admittance as a function of frequency.

Figure 3. Tidal gravity residuals (solid line) and estimated polar motion (dotted line). A drift of 7.87 μGal/yr was added to the polar motion model for visual clarity.

Figure 4. Superconducting Gravimeter residuals versus FG5 determinations of gravity change. Residuals corrected for tides, polar motion, and linear drift. Circles represent data taken from the NOAA instrument; Squares from the NSF instrument.

Figure 5. Comparison of gravity residuals (solid line) with rainfall events (dotted line).

VAN DAM FRANCIS: CONTINUOUS GRAVITY MEASUREMENTS IN BOULDER, COLORADO
VAN DAM FRANCIS: CONTINUOUS GRAVITY MEASUREMENTS IN BOULDER, COLORADO

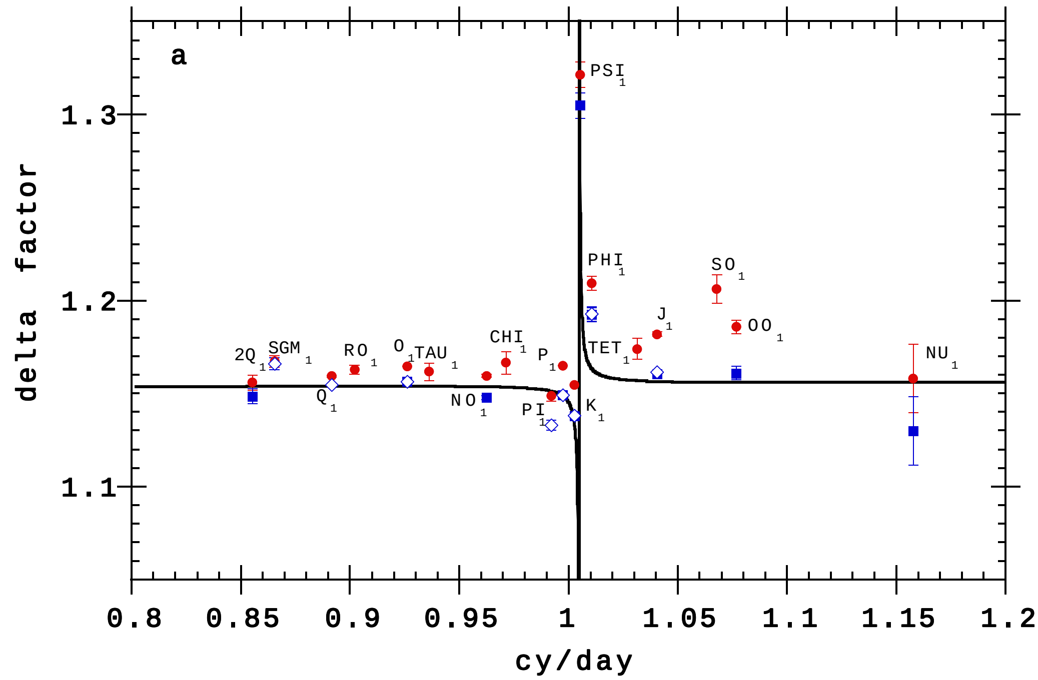
a
delta factor
cy/day
PSI 1
PHI 1
SO 1
OO 1
J 1
TET 1
NU 1
2Q 1
SGM 1
RO 1
O 1
TAU 1
CHI 1
P 1
Q 1
NO 1
PI 1
K 1
1.1
1.2
1.3
0.8
0.85
0.9
0.95
1
1.05
1.1
1.15
1.2

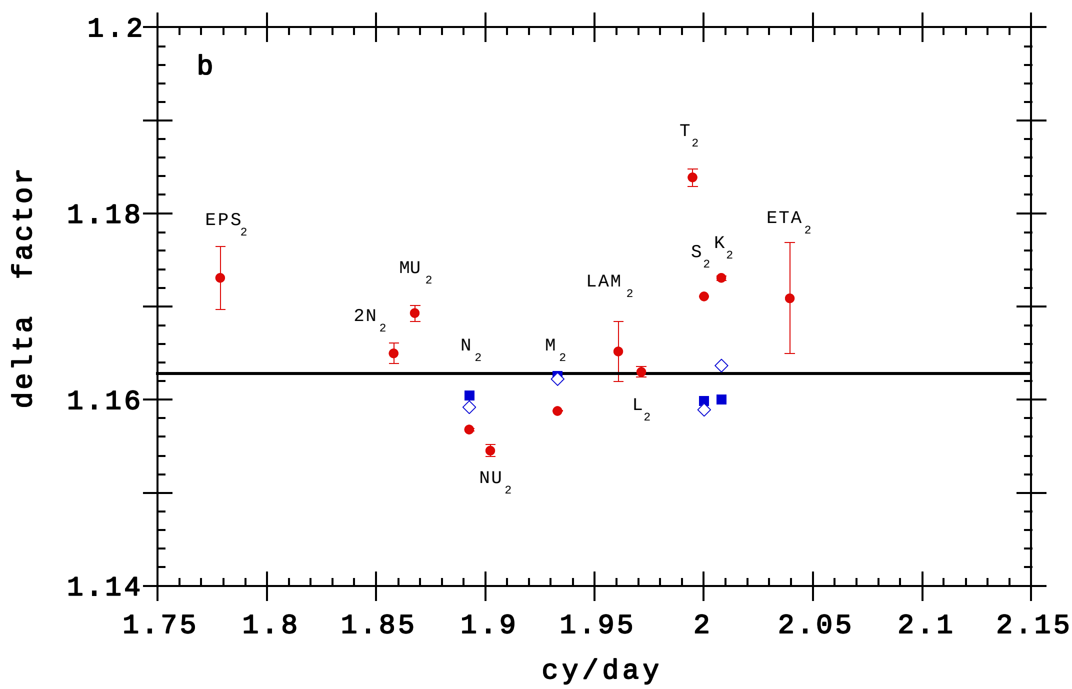
b
delta factor
cy/day
EPS 2
2N 2
MU 2
N 2
NU 2
M 2
LAM 2
L 2
T 2
S 2
K 2
ETA 2
1.14
1.16
1.18
1.2
1.75
1.8
1.85
1.9
1.95
2
2.05
2.1
2.15

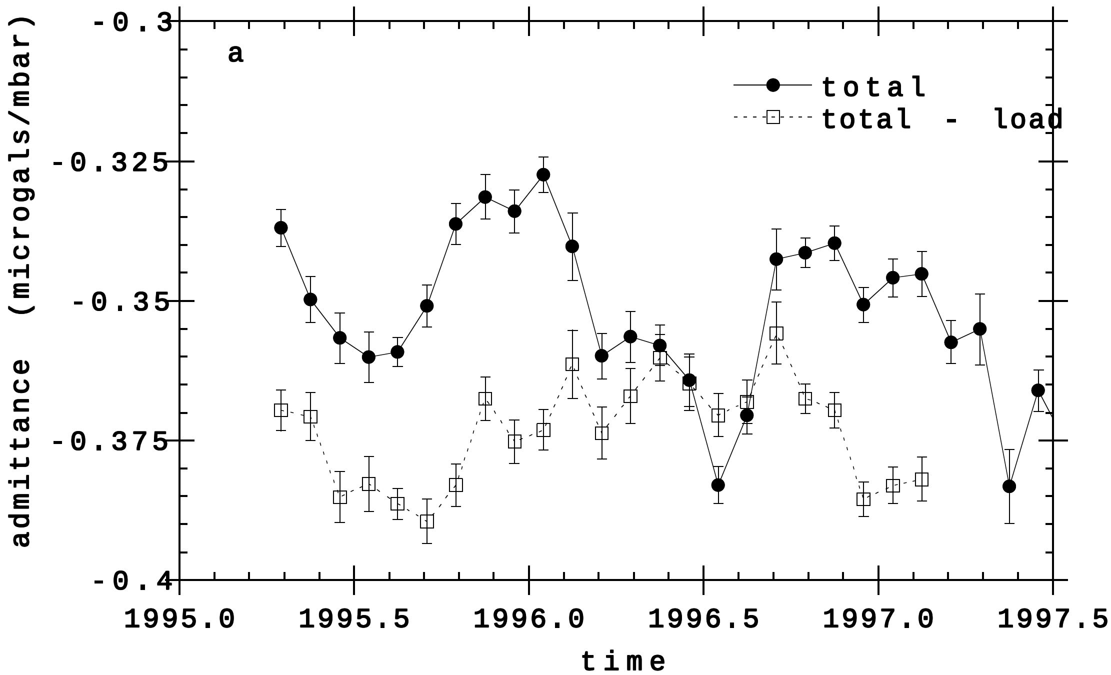

a
total
total - load
-0.3
-0.325
-0.35
-0.375
-0.4
admittance (microgals/mbar)
1995.0
1995.5
1996.0
1996.5
1997.0
1997.5
time

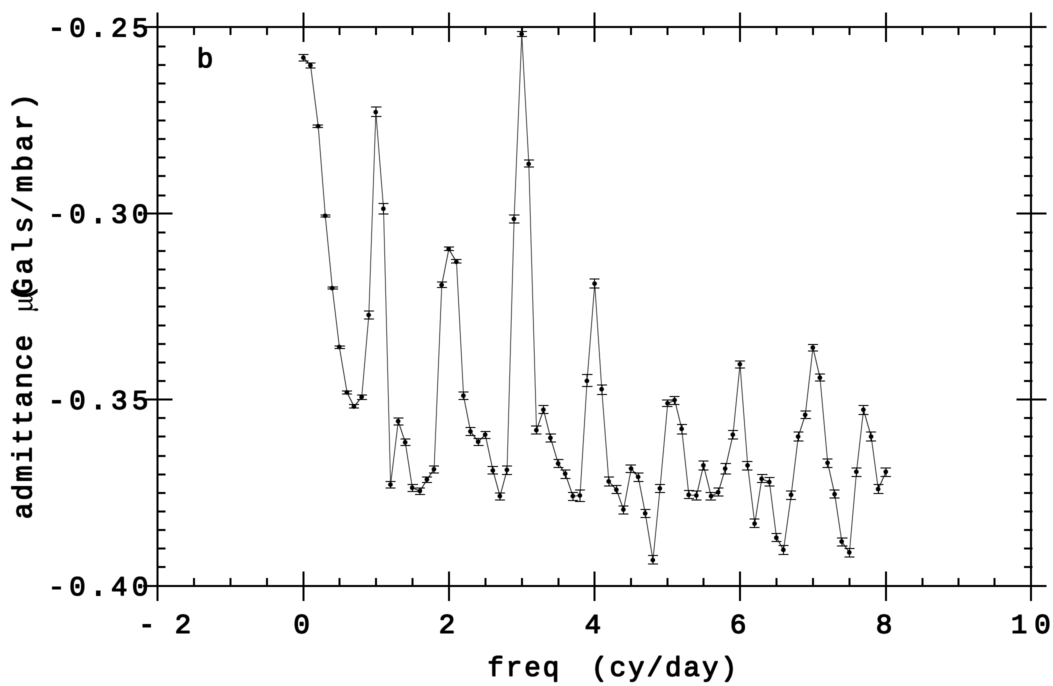

b
-0.25
-0.30
-0.35
-0.40
admittance μGals/mbar)
- 2
0
2
4
6
8
10
freq (cy/day)

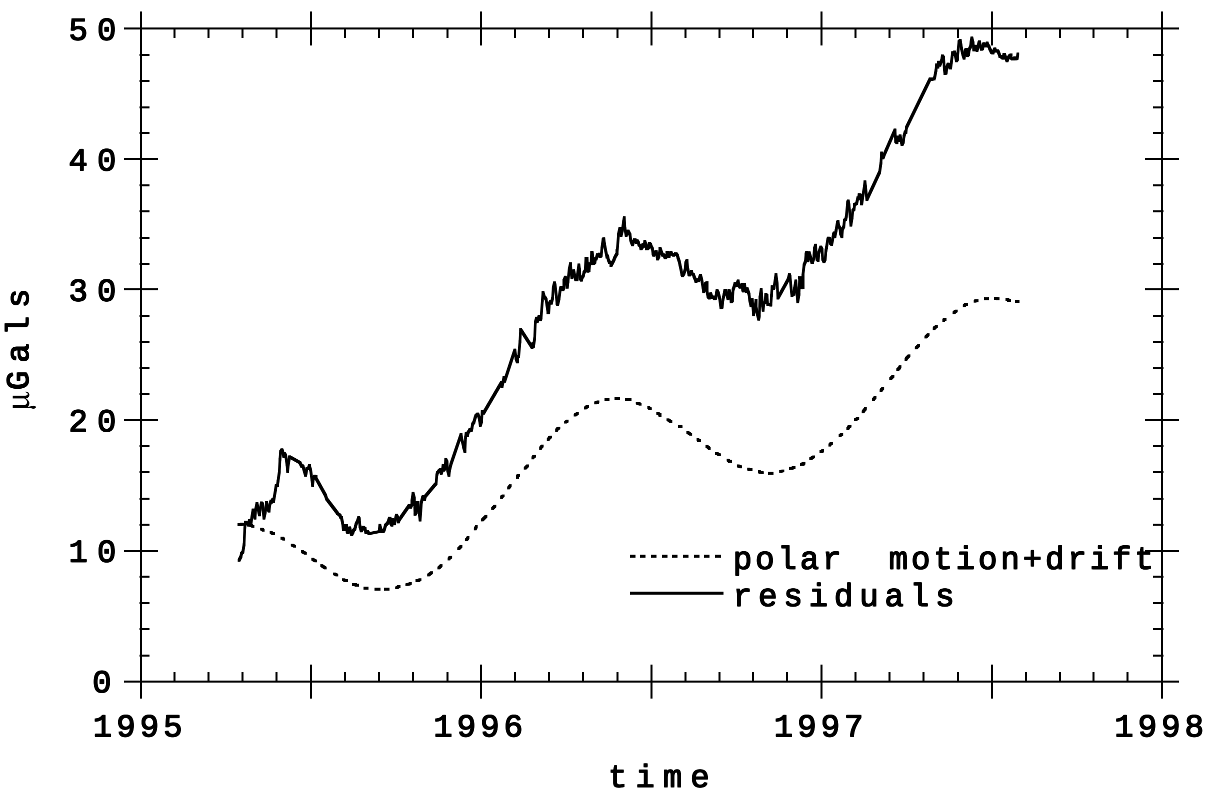

50
40
30
20
10
0
μGals
1995
1996
1997
1998
time
polar motion+drift
residuals

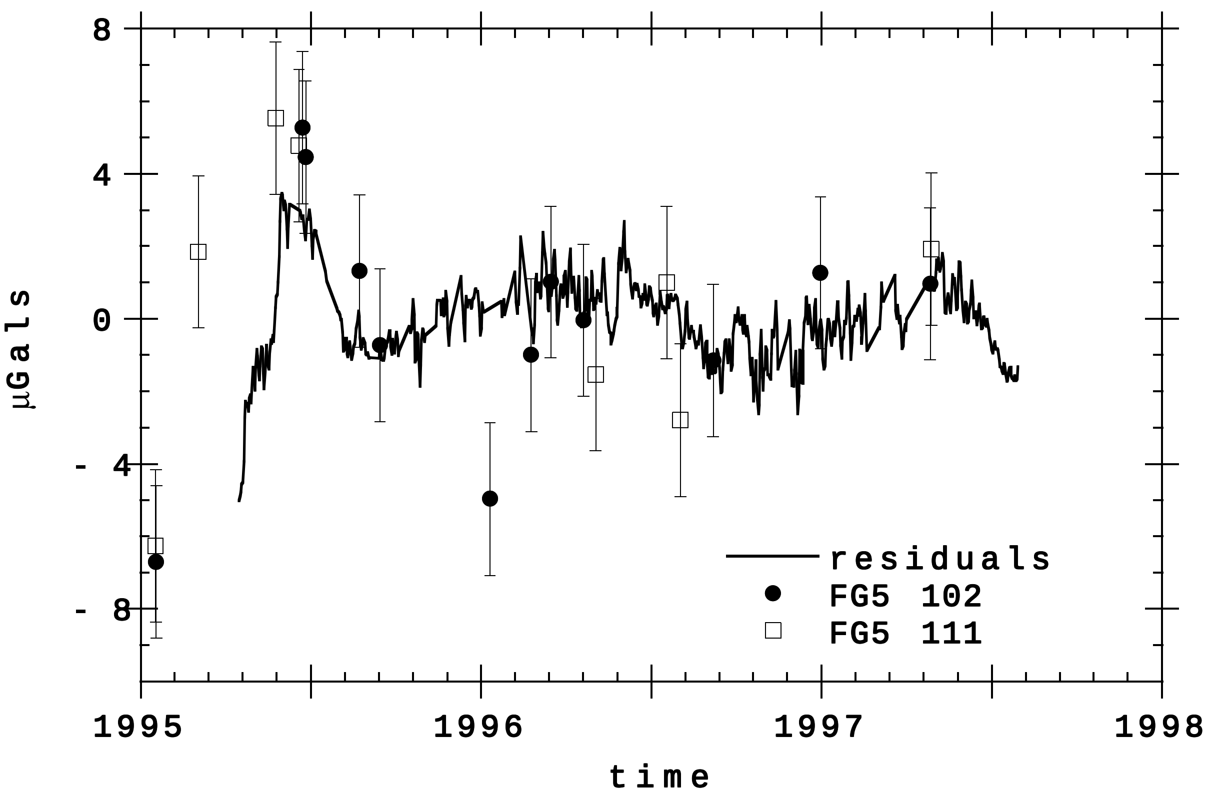

8
4
0
- 4
- 8
µGals
1995
1996
1997
1998
time
residuals
FG5 102
FG5 111

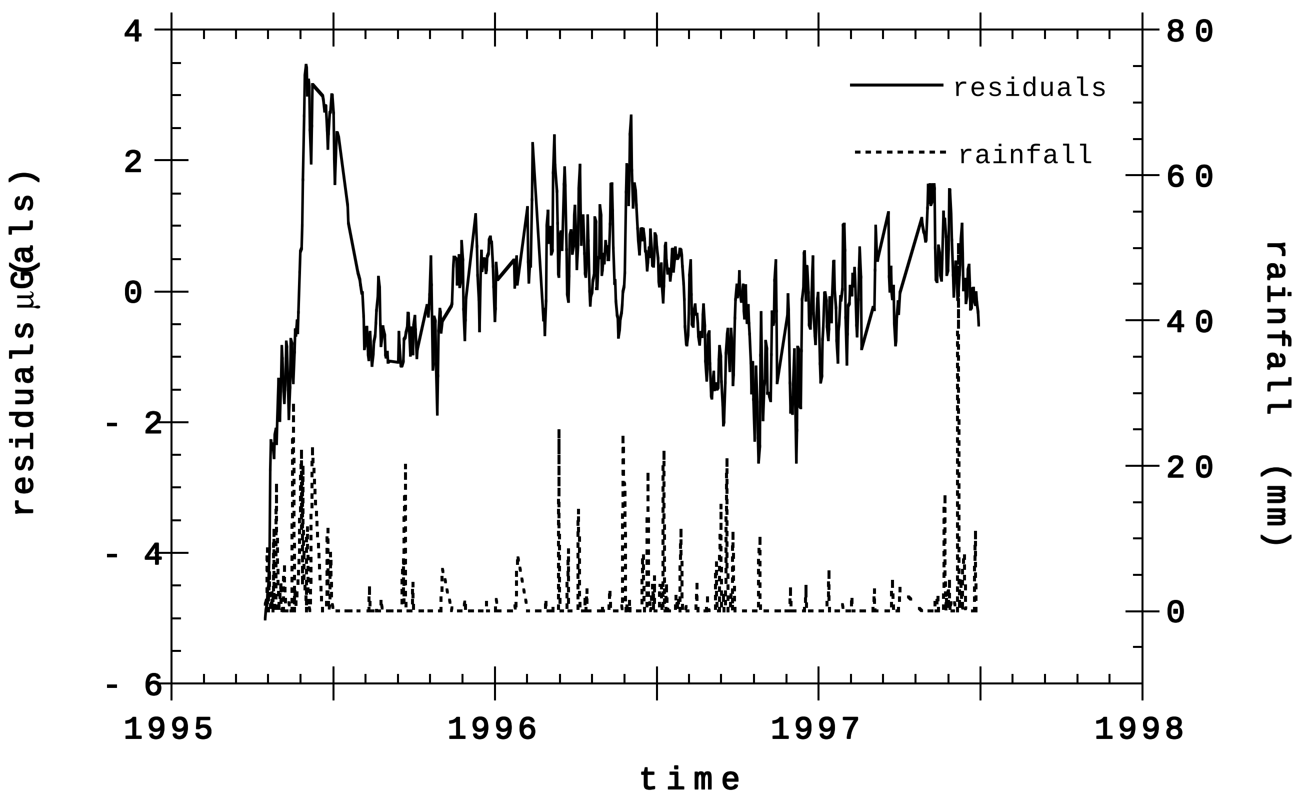
residuals
rainfall
residuals µGals)
rainfall (mm)
time
4
2
0
-2
-4
-6
80
60
40
20
0
1995
1996
1997
1998